Modeling of shell–beam transitions in the presence of finite rotations[1]

Werner Wagner

Institute for Structural Analysis, Universität Karlsruhe (TH)
Kaiserstr. 12, D–76131 Karlsruhe

Friedrich Gruttmann

Institute for Structural Analysis, Technische Universität Darmstadt
Alexanderstr. 7, D–64283 Darmstadt

A finite element formulation for a transition element between shells and beam structures is described in this paper. The elements should allow changes between models in an 'optimal' way without or with little disturbances which decrease rapidly due to the principle of Saint-Venant. Thus, the constraints are formulated in such a way that a transverse contraction within the coupling range is possible. The implementation of the coupling conditions is done with the Penalty Method or the Augmented Lagrange Method. The element formulation is derived for finite rotations. Same rotational formulations are used in beam and shell elements. Rotational increments up to an angle of 2π are possible without singularities based on a multiplicative update procedure. It can be shown that the transition to rigid bodies can be derived with some modifications. Examples prove the reliability of the transition formulation. Here simple element tests and practical applications are shown.

1. INTRODUCTION

The process of detailed modeling of thin-walled beam structures may lead to large systems and a complex numerical analysis. Even with modern computational equipment this task should be managed with problem oriented techniques. Parts of thin 3D-structures where only global behaviour is of interest can be discretized with beam elements whereas regions where for example local stability phenomena occur can be modeled with shell elements. Thus, transition elements have to be developed, which should combine both types of elements in a proper way. In general these elements are available in most of the commercial finite element codes. But simple examples show that they may lead to severe disturbances of the local stress state. This is especially important when considering material nonlinear behaviour.

2. FORMULATION OF CONSTRAINT EQUATIONS

The aim of this paper is to develop finite elements which describe the transition between shells and 3D-beams in such a way that the constraints imposed on both formulations are minimal. The description should hold for any case of geometrical nonlinearities. Therefore the elements have to be able to describe finite rotations. As basic kinematic assumption for the element we assume
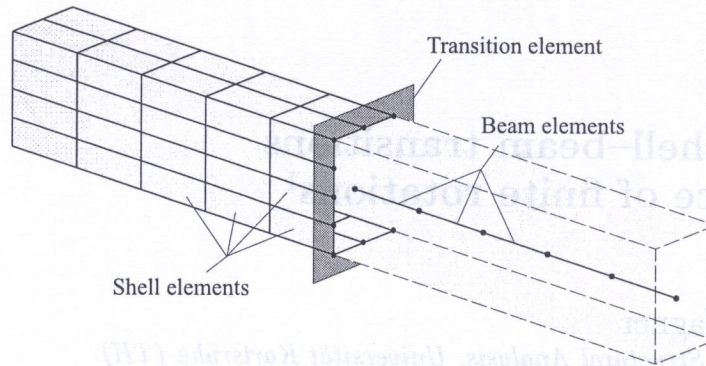

Fig. 1. Example: cross section of an U-shaped beam with shell and beam discretization
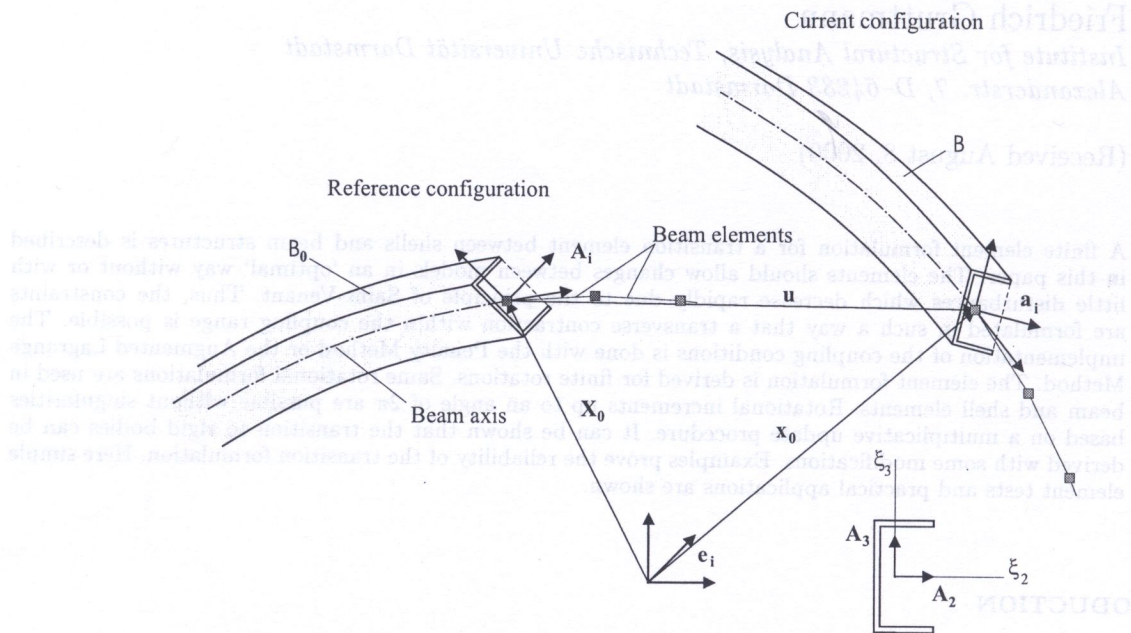

Fig. 2. Reference and current configuration of the cross section at transition

- an undeformable plane cross section in accordance with the beam theory. No warping effects are allowed (this may be defined for the beam element by default whereas it has to be enforced for the shell element as constraint).

- All nodes of the shell discretization which have to be coupled as well as the beam node are situated in this plane, see Fig. 1.

- All nodes in the cross section can move on a straight line through the center of gravity. (In a beam theory with elastic material behaviour we assume $\sigma_y = \sigma_z \approx 0$, which leads to $\varepsilon_x = \frac{\sigma_x}{E}$, $\varepsilon_y = -\nu\varepsilon_x$, $\varepsilon_z = -\nu\varepsilon_x$. Thus, an arbitrary point of the cross section can move only on a straight line through the center of gravity.)

Points on the cross section can be described by a convective coordinate system ξ_2, ξ_3 with base vectors $\mathbf{A}_2$, $\mathbf{A}_3$ in the undeformed and $\mathbf{a}_2$, $\mathbf{a}_3$ in the deformed configuration, see Fig. 2. Here the orthonormal base systems,

$$\mathbf{A}_i = \mathbf{R}_0\,\mathbf{e}_i = (\mathbf{A}_i \otimes \mathbf{e}_i)\,\mathbf{e}_i\,,$$

$$\mathbf{a}_i = \mathbf{R}\,\mathbf{e}_i = (\mathbf{a}_i \otimes \mathbf{e}_i)\,\mathbf{e}_i = \Delta\mathbf{R}\,\mathbf{R}_0\,\mathbf{e}_i\,,$$

$$\tag{1}$$

are introduced. Beam elements based on Bernoulli theory or Timoshenko theory can be used.

In the undeformed configuration an arbitrary point I of the cross section is defined by

$$\mathbf{X}_I = \mathbf{X}_0 + \xi_2\,\mathbf{A}_2 + \xi_3\,\mathbf{A}_3 . \tag{2}$$

The coordinates of this point $I\,(0, \xi_2, \xi_3)$ on the cross section can be calculated using the base vectors $\mathbf{A}_i$,

$$\xi_2 = (\mathbf{X}_I - \mathbf{X}_0)\cdot\mathbf{A}_2 , \qquad \xi_3 = (\mathbf{X}_I - \mathbf{X}_0)\cdot\mathbf{A}_3 . \tag{3}$$

An arbitrary point I of the cross section in the current configuration is found if

$$\mathbf{x}_I = \mathbf{x}_0 + c_2\mathbf{a}_2 + c_3\mathbf{a}_3 , \qquad c_2, c_3 \in \mathcal{R} \tag{4}$$

holds.

Due to the fact that points move on a straight line through the center of gravity (S) during the deformation the position of this point can be described using a parameter λ

$$\mathbf{x}_I = \mathbf{x}_0 + \lambda(\xi_2\,\mathbf{a}_2 + \xi_3\,\mathbf{a}_3), \qquad \lambda \in \mathcal{R}. \tag{5}$$

Here, λ can be defined from the distance between S and I in the undeformed and current configuration,

$$\lambda = \frac{\|\mathbf{x}_I - \mathbf{x}_0\|}{\|\mathbf{X}_I - \mathbf{X}_0\|} . \tag{6}$$

Thus, the following constraint equation holds for each point of the shell cross section

$$\mathbf{f} = \mathbf{x}_I - \mathbf{x}_0 - \lambda(\xi_2\,\mathbf{a}_2 + \xi_3\,\mathbf{a}_3) = \mathbf{0}. \tag{7}$$

Based on the above defined assumptions warping cannot be decribed. This may be crucial in some situations.

3. FINITE ELEMENT FORMULATION

Based on the above described kinematical assumptions the element is developed. The beam node in the transition cross-section is called 'reference node'. Furthermore, the base vectors $\mathbf{A}_2$ and $\mathbf{A}_3$ define the orientation of the cross section. It is assumed that the shell nodes to couple ('coupling nodes') lie in this plane. The vectors $\mathbf{A}_2$ and $\mathbf{A}_3$ are used to specify the section coordinates, see Eq. (3). In the current configuration the base vectors $\mathbf{a}_2$ und $\mathbf{a}_3$ of the beam element together with the convective coordinates $(0, \xi_2, \xi_3)$ and the parameter λ define the coupling nodes.

The mechanical model of the cross section can be considered as a sum of rigid beams which allow only for axial deflections. The boundary conditions are clamped at the reference node and jointed at the coupling node, see Fig. 3.

The implementation of the constraint equation (7) in a transition element is done via the Penalty and the Augmented Lagrange Method. Furthermore a consistent linearization is derived for the element with respect to finite rotations. The transition is formulated between an arbitrary shell node and the associated beam node as a two node element. Thus Fig. 3 may be interpreted as the system of all necessary transition elements for the shown case. The unknown values at both nodes of the element are introduced in the following vector,

$$\mathbf{v}^{(e)} = \begin{bmatrix} \mathbf{u}_I \\ \boldsymbol{\omega}_I \\ \mathbf{u}_0 \\ \boldsymbol{\omega}_0 \end{bmatrix}^{(e)}, \tag{8}$$
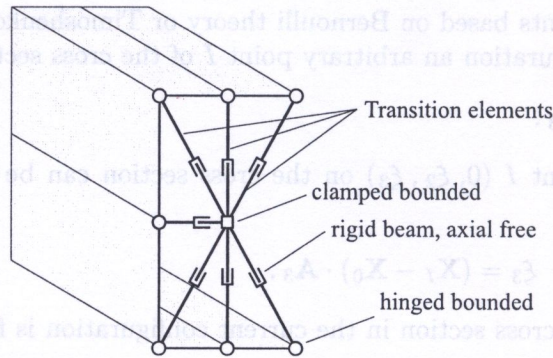
Fig. 3. Transition elements in a beam cross-section

where **u** are the displacements and $\boldsymbol{\omega}$ are the rotational quantities. The index '0' refers to the beam node whereas the index 'I' is used for the coupled shell node.

The equations of the penalty method, see e.g. [1, 6], are summarized in the following,

$$\Pi_P = \Pi(\mathbf{u}) + \widetilde{\Pi} = \Pi(\mathbf{u}) + \frac{1}{2}\alpha\,\mathbf{f}^T\mathbf{f}, \qquad \alpha \in \mathcal{R},$$

$$\delta\Pi_P = \delta\Pi(\mathbf{u}) + \delta\widetilde{\Pi} = \delta\Pi(\mathbf{u}) + \alpha\,\delta\mathbf{f}^T\mathbf{f}, \tag{9}$$

$$\Delta\delta\Pi_P = \Delta\delta\Pi(\mathbf{u}) + \Delta\delta\widetilde{\Pi} = \Delta\delta\Pi(\mathbf{u}) + \alpha\,\delta\mathbf{f}^T\Delta\mathbf{f} + \alpha\Delta\delta\mathbf{f}^T\mathbf{f}.$$

A more stable method is introduced by the Augmented Lagrange Method, see e.g. [4, 7, 8], with the following equations.

$$\Pi_A = \Pi(\mathbf{u}) + \widetilde{\Pi} = \Pi(\mathbf{u}) + \frac{1}{2}\alpha\,\mathbf{f}^T\mathbf{f} + \mathbf{\Lambda}^T\mathbf{f},$$

$$\delta\Pi_A = \delta\Pi(\mathbf{u}) + \delta\widetilde{\Pi} = \delta\Pi(\mathbf{u}) + \delta\mathbf{f}^T(\alpha\,\mathbf{f} + \mathbf{\Lambda}), \tag{10}$$

$$\Delta\delta\Pi_A = \Delta\delta\Pi(\mathbf{u}) + \Delta\delta\widetilde{\Pi} = \Delta\delta\Pi(\mathbf{u}) + \alpha\,\delta\mathbf{f}^T\Delta\mathbf{f} + \Delta\delta\mathbf{f}\,(\alpha\,\mathbf{f} + \mathbf{\Lambda}).$$

Here, α is the Penalty parameter which has to be chosen and $\mathbf{\Lambda}$ are the Lagrangian multipliers. These are held constant within an iteration step. The update reads

$$\mathbf{\Lambda}_{i+1} = \alpha\,\mathbf{f}_i + \mathbf{\Lambda}_i \quad \text{with} \quad \mathbf{\Lambda}_0 = \mathbf{0} \tag{11}$$

To derive the necessary equations for both methods simultaneously we introduce the vector $\widetilde{\mathbf{\Lambda}}$ with

$$\widetilde{\mathbf{\Lambda}} = \alpha\,\mathbf{f} \quad \text{(Penalty)}, \qquad \widetilde{\mathbf{\Lambda}} = \alpha\,\mathbf{f} + \mathbf{\Lambda} \quad \text{(Augmented Lagrange)}. \tag{12}$$

To determine the residual and the stiffness matrix we need to specify the variation and linearization of the constraints. If we denote the position vector from the reference node to the coupling node with respect to the basis $\mathbf{a}_i$ with

$$\mathbf{r}_I = \xi_2\,\mathbf{a}_2 + \xi_3\,\mathbf{a}_3, \tag{13}$$

it holds for

$$\mathbf{f} = \mathbf{x}_I - \mathbf{x}_0 - \lambda\mathbf{r}_I \tag{14}$$

and its variation

$$\delta\mathbf{f} = \delta\mathbf{u}_I - \delta\mathbf{u}_0 - \delta\lambda\,\mathbf{r}_I - \lambda\,\delta\mathbf{r}_I. \tag{15}$$

Here $\delta\lambda$ and $\delta\mathbf{r}_I$ have to be derived. We introduce the distance R of the nodes in the reference state

$$R = \|\mathbf{X}_I - \mathbf{X}_0\|. \tag{16}$$

In the current configuration the distance of these nodes is defined by

$$\|\mathbf{x}_I - \mathbf{x}_0\| = \sqrt{(\mathbf{x}_I - \mathbf{x}_0) \cdot (\mathbf{x}_I - \mathbf{x}_0)}. \tag{17}$$

Starting from Eq. (6) and using the chain rule and product rule it holds for $\delta\lambda$

$$\delta\lambda = \frac{1}{R} \frac{(\delta\mathbf{u}_I - \delta\mathbf{u}_0) \cdot (\mathbf{x}_I - \mathbf{x}_0) + (\mathbf{x}_I - \mathbf{x}_0) \cdot (\delta\mathbf{u}_I - \delta\mathbf{u}_0)}{2\sqrt{(\mathbf{x}_I - \mathbf{x}_0) \cdot (\mathbf{x}_I - \mathbf{x}_0)}},$$

$$\delta\lambda = \frac{1}{R} \frac{\mathbf{x}_I - \mathbf{x}_0}{\|\mathbf{x}_I - \mathbf{x}_0\|} \cdot (\delta\mathbf{u}_I - \delta\mathbf{u}_0). \tag{18}$$

With the abbreviations

$$\mathbf{n} = \frac{\mathbf{x}_I - \mathbf{x}_0}{\|\mathbf{x}_I - \mathbf{x}_0\|} \quad \text{and} \quad \hat{\mathbf{n}} = \frac{1}{R}\,\mathbf{n}, \tag{19}$$

$\delta\lambda$ can be written finally as

$$\delta\lambda = \hat{\mathbf{n}} \cdot (\delta\mathbf{u}_I - \delta\mathbf{u}_0). \tag{20}$$

The second term to be derived is the variation $\delta\mathbf{r}_I$. With

$$\delta\mathbf{r}_I = \xi_2\,\delta\mathbf{a}_2 + \xi_3\,\delta\mathbf{a}_3 \tag{21}$$

and

$$\delta\mathbf{a}_i = \delta\boldsymbol{\omega}_0 \times \mathbf{a}_i, \tag{22}$$

$\delta\mathbf{r}_I$ can be stated as

$$\delta\mathbf{r}_I = \xi_2\,\delta\boldsymbol{\omega}_0 \times \mathbf{a}_2 + \xi_3\,\delta\boldsymbol{\omega}_0 \times \mathbf{a}_3. \tag{23}$$

Thus, $\delta\mathbf{r}_I$ is defined in terms of $\mathbf{r}_I$ and $\delta\boldsymbol{\omega}_0$

$$\delta\mathbf{r}_I = \delta\boldsymbol{\omega}_0 \times \mathbf{r}_I = \mathbf{W}\,\delta\boldsymbol{\omega}_0 \tag{24}$$

with

$$\mathbf{W} = -\operatorname{skew}\mathbf{r}_I = \begin{bmatrix} 0 & r_{3I} & -r_{2I} \\ -r_{3I} & 0 & r_{1I} \\ r_{2I} & -r_{1I} & 0 \end{bmatrix}. \tag{25}$$

The axial vector $\boldsymbol{\omega}_0$ contains the rotational degrees of freedom of the reference node.

Finally the variation of the constraint can be written as

$$\begin{aligned} \delta\mathbf{f} &= \delta\mathbf{u}_I - \delta\mathbf{u}_0 - [\hat{\mathbf{n}} \cdot (\delta\mathbf{u}_I - \delta\mathbf{u}_0)]\mathbf{r}_I - \lambda\mathbf{W}\,\delta\boldsymbol{\omega}_0 \\ &= (\mathbf{1} - \mathbf{r}_I \otimes \hat{\mathbf{n}})(\delta\mathbf{u}_I - \delta\mathbf{u}_0) - \lambda\mathbf{W}\,\delta\boldsymbol{\omega}_0 \\ &= \mathbf{A}(\delta\mathbf{u}_I - \delta\mathbf{u}_0) - \lambda\mathbf{W}\,\delta\boldsymbol{\omega}_0 \end{aligned} \tag{26}$$

with

$$\mathbf{A} = \mathbf{1} - \mathbf{r}_I \otimes \hat{\mathbf{n}}. \tag{27}$$

Thus, the residual for a single transition element is defined by

$$\delta\widetilde{\Pi}^{(e)} = \delta\mathbf{v}^{T(e)}\,\mathbf{G}^{(e)} = \delta\mathbf{v}^{T(e)}\,\mathbf{B}_f^T\,\tilde{\mathbf{\Lambda}} = \begin{bmatrix} \delta\mathbf{u}_I^T,\ \delta\boldsymbol{\omega}_I^T,\ \delta\mathbf{u}_0^T,\ \delta\boldsymbol{\omega}_0^T \end{bmatrix}^{(e)} \begin{bmatrix} \mathbf{A}^T \\ \mathbf{0} \\ -\mathbf{A}^T \\ -\lambda\mathbf{W}^T \end{bmatrix} \tilde{\mathbf{\Lambda}}\,. \tag{28}$$

The necessary terms in Eqs. (9)$_3$, (10)$_3$ are derived in a similar way and the tangent stiffness matrix follows from

$$\mathbf{k}_T^{(e)} = \mathbf{B}_f^T\,\alpha\,\mathbf{B}_f + \begin{bmatrix} \bar{\mathbf{P}} & \mathbf{0} & -\bar{\mathbf{P}} & -\mathbf{F}^T \\ \mathbf{0} & \mathbf{0} & \mathbf{0} & \mathbf{0} \\ -\bar{\mathbf{P}} & \mathbf{0} & \bar{\mathbf{P}} & \mathbf{F}^T \\ -\mathbf{F} & \mathbf{0} & \mathbf{F} & \mathbf{H} \end{bmatrix} \tag{29}$$

with

$$\begin{aligned}
\bar{\mathbf{P}} &= -(\tilde{\mathbf{\Lambda}}\cdot\mathbf{r}_I)\,\hat{\mathbf{P}}\,, \\
\hat{\mathbf{P}} &= \frac{1}{R}\,\frac{1}{\|\mathbf{x}_I - \mathbf{x}_0\|}\,[\mathbf{1} - (\mathbf{n}\otimes\mathbf{n})]\,, \\
\mathbf{F} &= (\mathbf{r}_I \times \tilde{\mathbf{\Lambda}})\otimes\hat{\mathbf{n}}\,, \\
\mathbf{H} &= -\lambda\left[\frac{1}{2}(\mathbf{r}_I\otimes\tilde{\mathbf{\Lambda}} + \tilde{\mathbf{\Lambda}}\otimes\mathbf{r}_I) - (\tilde{\mathbf{\Lambda}}\cdot\mathbf{r}_I)\mathbf{1}\right].
\end{aligned} \tag{30}$$

4. RIGID BODY TRANSITION ELEMENT

In the following we discuss the application of the above derived equations on the transition between rigid and flexible parts of structures. The deformation of a rigid body is described by the translation and the rotation of a reference point '0'. Any other points on the rigid body can be described by a convective coordinate system ξ_1, ξ_2, ξ_3 with base vectors $\mathbf{A}_1$, $\mathbf{A}_2$, $\mathbf{A}_3$ in the undeformed and $\mathbf{a}_1$, $\mathbf{a}_2$, $\mathbf{a}_3$ in the deformed configuration, see Eqs. (2) and (3). Furthermore the same orthonormal base systems $\mathbf{A}_i$ and $\mathbf{a}_i$ (Eq. (1)) are used. These other points may be points were a transition to flexible parts (for example a shell) of the structure occur. It holds for the current configuration, see Eqs. (5), (13)

$$\mathbf{x}_I = \mathbf{x}_0 + (\xi_1\,\mathbf{a}_1 + \xi_2\,\mathbf{a}_2 + \xi_3\,\mathbf{a}_3) = \mathbf{x}_0 + \mathbf{r}_I \tag{31}$$

and the constraint is defined by, see Eq. (7)

$$\mathbf{f} = \mathbf{x}_I - \mathbf{x}_0 - (\xi_1\,\mathbf{a}_1 + \xi_2\,\mathbf{a}_2 + \xi_3\,\mathbf{a}_3) = (\mathbf{X}_I + \mathbf{u}_I) - (\mathbf{X}_0 + \mathbf{u}_0) - \mathbf{r}_I = \mathbf{0}. \tag{32}$$

Thus, the equations derived in Sections 2 and 3 can be used with $\lambda = 1$.

With $\delta\mathbf{r}_I = \delta\boldsymbol{\omega}_0 \times \mathbf{r}_I = \mathbf{W}\,\delta\boldsymbol{\omega}_0$, see Eqs. (24)–(25), the variation of the constraint yields

$$\delta\mathbf{f} = \delta\mathbf{u}_I - \delta\mathbf{u}_0 - \delta\mathbf{r}_I = \delta\mathbf{u}_I - \delta\mathbf{u}_0 - \mathbf{W}\,\delta\boldsymbol{\omega}_0\,. \tag{33}$$

Finally the residual for a single transition element is

$$\mathbf{G}^{(e)} = \mathbf{B}_f^T\,\tilde{\mathbf{\Lambda}} = \begin{bmatrix} \mathbf{1} \\ \mathbf{0} \\ -\mathbf{1} \\ -\mathbf{W}^T \end{bmatrix} \tilde{\mathbf{\Lambda}}\,. \tag{34}$$
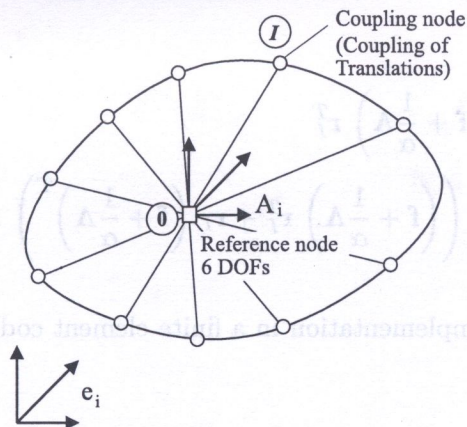
Fig. 4. Transition between rigid and flexible parts of a structure

The mechanical model of the transition between rigid and flexible parts is now interpretable as a sum of pure rigid beam elements with clamped boundary conditions at the reference node and jointed boundary conditions at the coupling nodes, see Fig. 4.

Next we derive the necessary linearization for the transition element. Similar to $\delta \mathbf{f}$ the linearization $\Delta \mathbf{f}$ can be written as

$$\Delta \mathbf{f} = \mathbf{B}_f \, \Delta \mathbf{v}^{(e)} = \begin{bmatrix} \mathbf{1} & \mathbf{0} & -\mathbf{1} & -\mathbf{W} \end{bmatrix} \begin{bmatrix} \Delta \mathbf{u}_I \\ \Delta \boldsymbol{\omega}_I \\ \Delta \mathbf{u}_0 \\ \Delta \boldsymbol{\omega}_0 \end{bmatrix}. \tag{35}$$

Furthermore the term $\Delta \delta \mathbf{f}$ has to be derived:

$$\Delta \delta \mathbf{f} = -\Delta \delta \mathbf{r}_I = -(\xi_1 \, \Delta \delta \mathbf{a}_1 + \xi_2 \, \Delta \delta \mathbf{a}_2 + \xi_3 \, \Delta \delta \mathbf{a}_3) \tag{36}$$

with

$$\Delta \delta \mathbf{a}_i = \delta \boldsymbol{\omega}_0 \times \Delta \mathbf{a}_i = \delta \boldsymbol{\omega}_0 \times (\Delta \boldsymbol{\omega}_0 \times \mathbf{a}_i)$$

$$= (\delta \boldsymbol{\omega}_0 \cdot \mathbf{a}_i) \, \Delta \boldsymbol{\omega}_0 - (\delta \boldsymbol{\omega}_0 \cdot \Delta \boldsymbol{\omega}_0) \, \mathbf{a}_i = (\delta \boldsymbol{\omega}_0 \otimes \Delta \boldsymbol{\omega}_0) \, \mathbf{a}_i - (\delta \boldsymbol{\omega}_0 \cdot \Delta \boldsymbol{\omega}_0) \, \mathbf{a}_i, \tag{37}$$

which finally leads to

$$\Delta \delta \mathbf{f} = -\left[(\delta \boldsymbol{\omega}_0 \otimes \Delta \boldsymbol{\omega}_0) - (\delta \boldsymbol{\omega}_0 \cdot \Delta \boldsymbol{\omega}_0) \, \mathbf{1} \right] \mathbf{r}_I. \tag{38}$$

Thus, the term $\Delta \delta \mathbf{f}^T (\alpha \mathbf{f} + \boldsymbol{\Lambda})$ for the linearization is given by

$$\Delta \delta \mathbf{f}^T (\alpha \mathbf{f} + \boldsymbol{\Lambda}) = -(\alpha \mathbf{f} + \boldsymbol{\Lambda})^T \left[(\delta \boldsymbol{\omega}_0 \otimes \Delta \boldsymbol{\omega}_0) - (\delta \boldsymbol{\omega}_0 \cdot \Delta \boldsymbol{\omega}_0) \, \mathbf{1} \right] \mathbf{r}_I$$

$$= -(\alpha \mathbf{f} + \boldsymbol{\Lambda})^T \left[(\Delta \boldsymbol{\omega}_0 \cdot \mathbf{r}_I) \, \delta \boldsymbol{\omega}_0 - (\delta \boldsymbol{\omega}_0 \cdot \Delta \boldsymbol{\omega}_0) \, \mathbf{r}_I \right]$$

$$= \delta \boldsymbol{\omega}_0^T \left(-(\alpha \mathbf{f} + \boldsymbol{\Lambda}) \, \mathbf{r}_I^T + (\alpha \mathbf{f} + \boldsymbol{\Lambda})^T \, \mathbf{r}_I \, \mathbf{1} \right) \Delta \boldsymbol{\omega}_0$$

$$= \delta \boldsymbol{\omega}_0^T \alpha \, \mathbf{H} \, \Delta \boldsymbol{\omega}_0 \tag{39}$$

and we end up with the associated tangent stiffness matrix on element level

$$\mathbf{k}_T^{(e)} = \alpha \begin{bmatrix} \mathbf{1} & \mathbf{0} & -\mathbf{1} & -\mathbf{W} \\ \mathbf{0} & \mathbf{0} & \mathbf{0} & \mathbf{0} \\ -\mathbf{1} & \mathbf{0} & \mathbf{1} & \mathbf{W} \\ -\mathbf{W}^T & \mathbf{0} & \mathbf{W}^T & \mathbf{W}^T \mathbf{W} + \mathbf{H} \end{bmatrix}. \tag{40}$$

with

$$\mathbf{H} = \left(\mathbf{f} + \frac{1}{\alpha}\boldsymbol{\Lambda}\right)^T \mathbf{r}_I \mathbf{1} - \left(\mathbf{f} + \frac{1}{\alpha}\boldsymbol{\Lambda}\right) \mathbf{r}_I^T$$

$$\approx \left(\mathbf{f} + \frac{1}{\alpha}\boldsymbol{\Lambda}\right)^T \mathbf{r}_I \mathbf{1} - \frac{1}{2}\left(\left(\mathbf{f} + \frac{1}{\alpha}\boldsymbol{\Lambda}\right)\mathbf{r}_I^T + \mathbf{r}_I \left(\mathbf{f} + \frac{1}{\alpha}\boldsymbol{\Lambda}\right)^T\right). \tag{41}$$

Now all equations for the implementation in a finite element code are derived.

5. EXAMPLES

The developed finite element formulations for both transition elements have been implemented in an enhanced version of the program FEAP, documented in a basic version in [10].

5.1. Clamped thin-walled H-beam

The first example demonstrates the effect of a rigid and soft transition element for the case of a clamped thin-walled H-beam under axial load. The first part of the beam is modeled with beam elements [2, 9], the second part is discretized using shell elements [3]. Geometry and material data are shown in Fig. 5. In Fig. 6 the transverse normal stresses are plotted for the shell region. It can be seen clearly that in the rigid case stresses occur due to obstruction of the transverse deformations. The magnitude of these stresses σ_{22} amounts to more than 20 % of the longitudinal stress σ_{11}, see Fig. 7.

The distribution of normal and transverse stresses along a line through the center of gravity is depicted in Fig. 7. It can be seen clearly that there is no disturbance of the stress state if the soft transition elements are used.
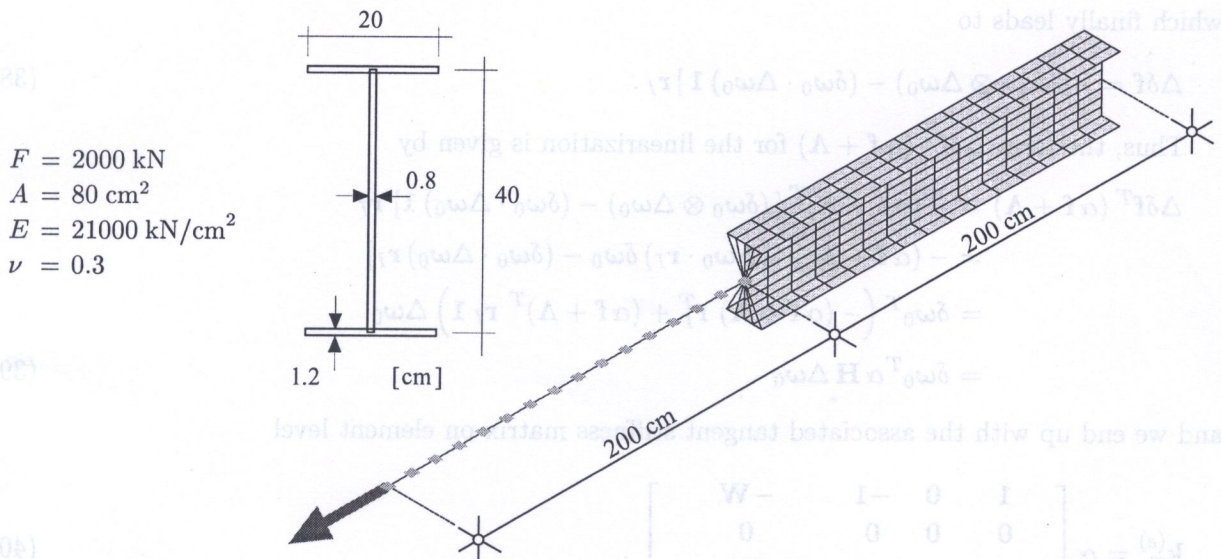
$F = 2000$ kN
$A = 80$ cm^2
$E = 21000$ kN/cm^2
$\nu = 0.3$

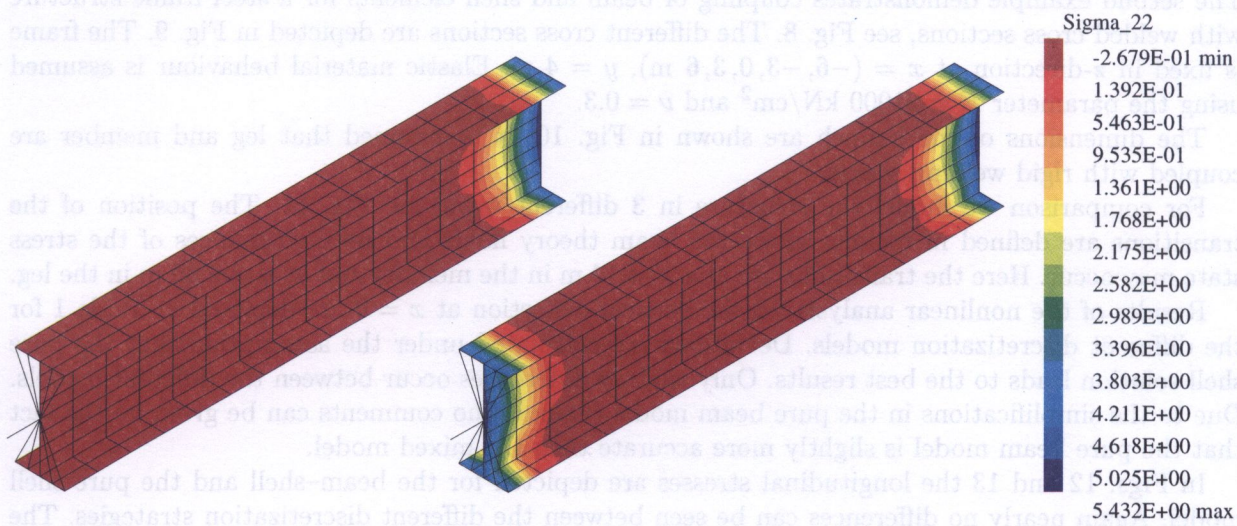**Fig. 5.** Clamped beam under axial load

Fig. 6. Transverse normal stresses for soft and rigid transition element
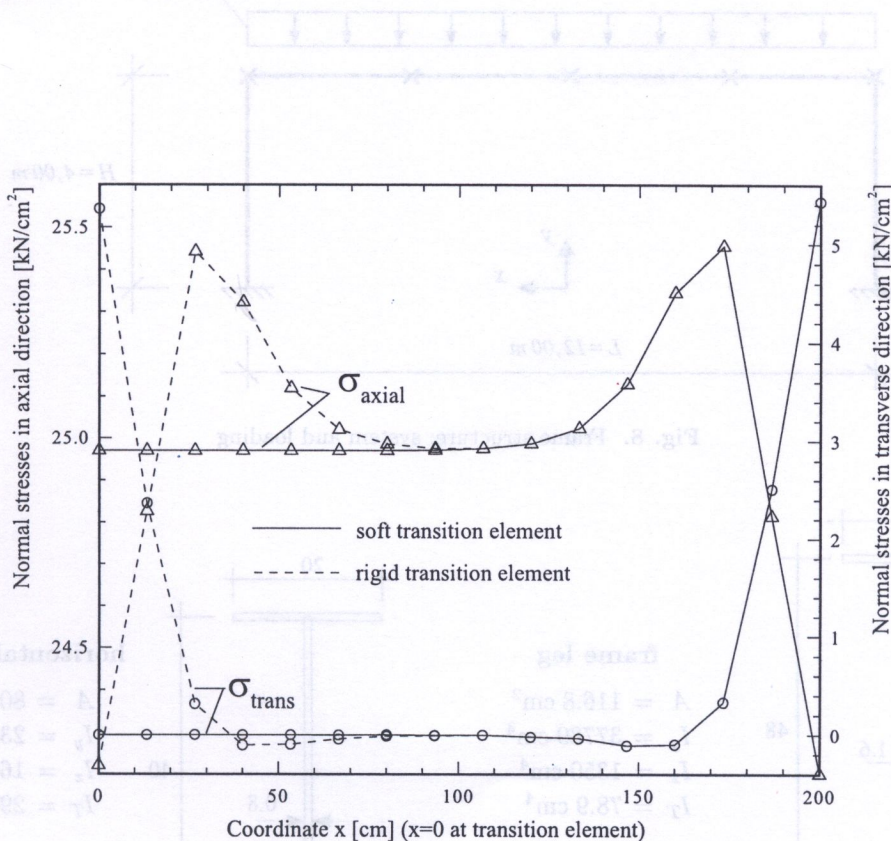

Fig. 7. Distribution of stresses along a line (coordinate x) through the center of gravity

5.2. Steel frame structure

The second example demonstrates coupling of beam and shell elements for a steel frame structure with welded cross sections, see Fig. 8. The different cross sections are depicted in Fig. 9. The frame is fixed in z-direction at $x = (-6, -3, 0, 3, 6$ m$)$, $y = 4$ m. Elastic material behaviour is assumed using the parameter $E = 21000$ kN/cm^2 and $\nu = 0.3$.

The dimensions of the haunch are shown in Fig. 10. It is assumed that leg and member are coupled with rigid welding seams.

For comparison we model the structure in 3 different ways, see Fig. 11. The position of the transitions are defined in regions where the beam theory holds and no disturbances of the stress state may occur. Here the transitions are at $x = 4.14$ m in the member and at $y = 2.60$ m in the leg.

Results of the nonlinear analysis for the vertical deflection at $x = 0$ are depicted in Table 1 for the different discretization models. Deviations are calculated under the assumption that the pure shell solution leads to the best results. Only slightly differences occur between the different models. Due to the simplifications in the pure beam model (haunch) no comments can be given on the fact that the pure beam model is slightly more accurate then the mixed model.

In Figs. 12 and 13 the longitudinal stresses are depicted for the beam–shell and the pure shell model. Again nearly no differences can be seen between the different discretization strategies. The maximum differences in the stresses σ_{11} are about 4% in the transition zone. Thus, the derived transition elements can be used efficiently in coupling these types of elements without nearly any disturbances of stress and deformation state.
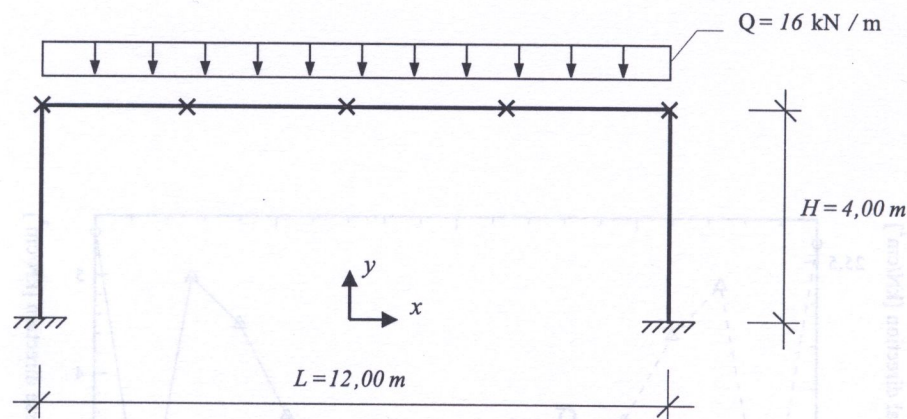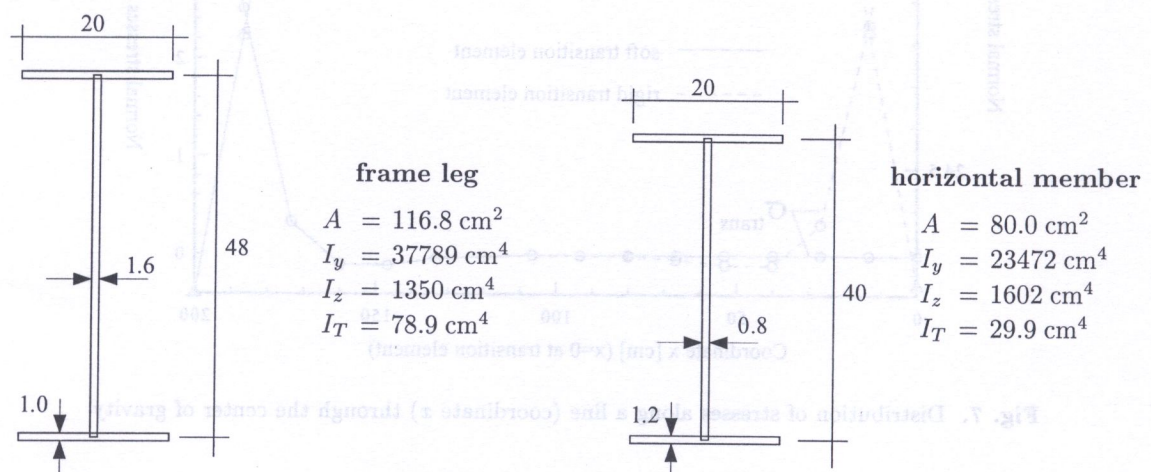

Fig. 8. Frame structure: system and loading

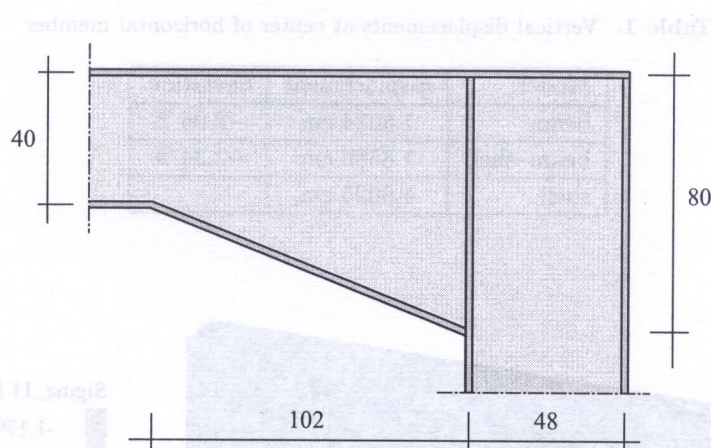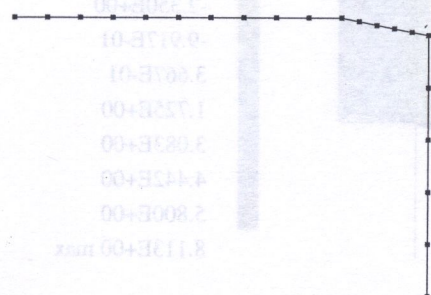**Fig. 9.** Definition of cross sections

Fig. 10. Definition of haunch, values in cm

Beam model

Here, 20 beam elements are used. Within the haunch 5 elements with constant cross sections are used.

Beam–shell model

For the shell part we use 720 shell elements whereas the beam part is modeled with 28 beam elements. At each transition 16 transition elements are used.
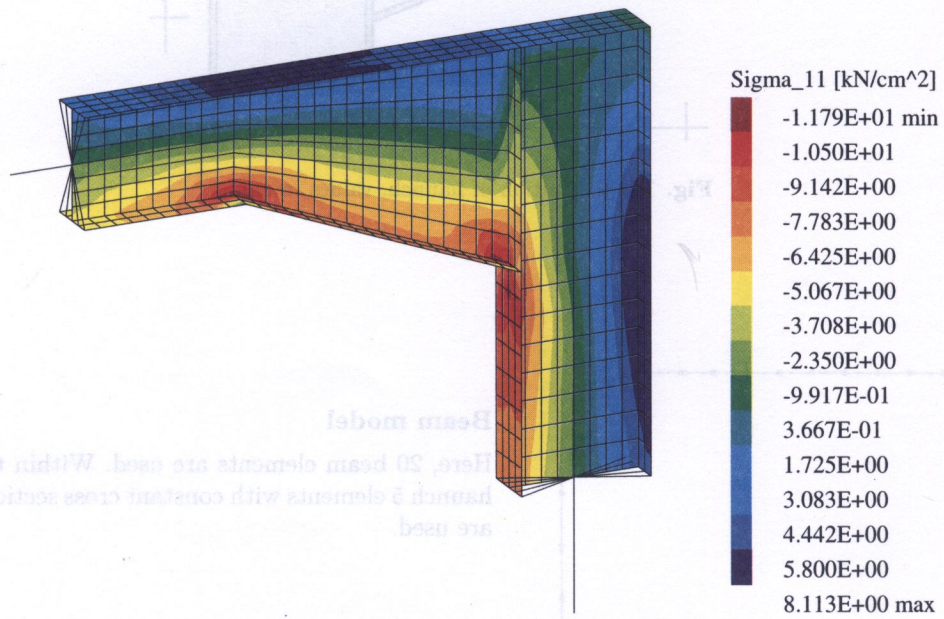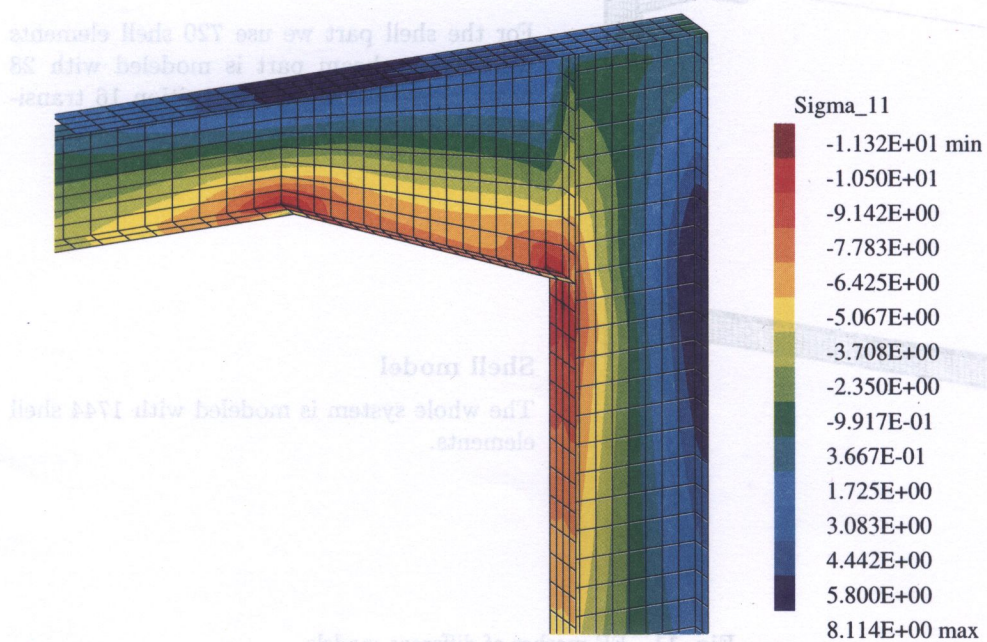
Shell model

The whole system is modeled with 1744 shell elements.

Fig. 11. FE-meshes of different models

Table 1. Vertical displacements at center of horizontal member

Model	displacement	deviation
beam	1.8634 cm	−2.06 %
beam−shell	1.8580 cm	−2.34 %
shell	1.9025 cm	−

Sigma_11 [kN/cm^2]

-1.179E+01 min
-1.050E+01
-9.142E+00
-7.783E+00
-6.425E+00
-5.067E+00
-3.708E+00
-2.350E+00
-9.917E-01
3.667E-01
1.725E+00
3.083E+00
4.442E+00
5.800E+00
8.113E+00 max

Fig. 12. Normal stresses, beam−shell model

Sigma_11

-1.132E+01 min
-1.050E+01
-9.142E+00
-7.783E+00
-6.425E+00
-5.067E+00
-3.708E+00
-2.350E+00
-9.917E-01
3.667E-01
1.725E+00
3.083E+00
4.442E+00
5.800E+00
8.114E+00 max

Fig. 13. Normal stresses, shell model

5.3. Clamped beam under end moment

In the third example we dicuss the modeling of a clamped beam under end moments using volume elements, e.g. [5]. Here, the question arises how to model the application of the end moment. A simple method is to model the beam tip with rigid transition elements. System and loading are shown in Fig. 14 whereas different deformed meshes and the material parameter are depicted in Fig. 15. No difficulies arise and the problem can be calculated using 5 incremental steps until a moment of $M = 2\pi\, EI/\ell$ which leads to a complete circle of the deformed mesh. Thus the transition elements describe the application of the moment on the volume elements correctly.

Fig. 14. Clamped beam under end moment

$$
\begin{aligned}
\ell &= 10 \\
b &= 1 \\
h &= 0.1 \\
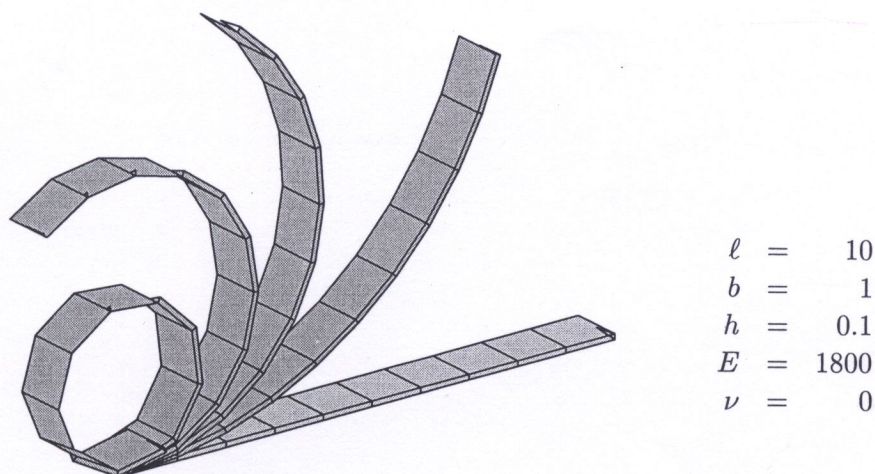E &= 1800 \\
\nu &= 0
\end{aligned}
$$
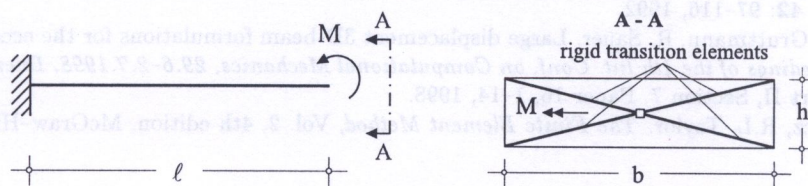
Fig. 15. Deformed meshes for clamped beam under end moment

6. CONCLUSIONS

A finite element formulation for a transition element between shells and beam structures has been described. The coupling condition is formulated such that transverse contraction within the transition range is possible. The element allows changes between models in an 'optimal' way without or with very little disturbances. The constraints are considered using either the Penalty Method or the Augmented Lagrange Method. A slightly modification leads to a formulation for the transition between rigid and flexible parts of structures. Examples show the efficiency and practical applicability of the derived transition elements.

REFERENCES

[1] C.A. Felippa. Error analysis of penalty function techniques for constraint definition in linear algebraic systems. *Int. J. Num. Methods Engng.*, **11**: 709–728, 1977.

[2] F. Gruttmann, R. Sauer, W. Wagner. A geometrical nonlinear eccentric 3D beam element with arbitrary cross-sections. *Comp. Methods Appl. Mech. Engrg.*, **160**: 383–400, 1998.

[3] F. Gruttmann , S. Klinkel, W. Wagner, A finite rotation shell theory with application to composite structures. *Europ. Journal of Finite Elements*, **4**: 597–632, 1995.

[4] M.R. Hestenes. Multiplier and gradient methods. *J. of Optimization Theory and Applications*, **4**: 303–320, 1969.

[5] S. Klinkel, F. Gruttmann, W. Wagner. A continuum based 3D-shell element for laminated structures. *Computers and Structures*, **71**: 43–62 1999.

[6] D.G. Luenberger. *Linear and Nonlinear Programming*, 2nd edition. Addison–Wesley, Reading, 1989.

[7] M.J.D. Powell, A method for nonlinear constraints and minimization problems. In: R. Fletcher, ed., *Optimization*, 283–298, 1969.

[8] J.C. Simo, T.A. Laursen. An augmented lagrangian treatment of contact problems involving friction. *Computers and Structures*, **42**: 97–116, 1992.

[9] W. Wagner, F. Gruttmann, R. Sauer. Large displacement 3D-beam formulations for the eccentric coupling with shells. In: *Proceedings of the 4th Int. Conf. on Computational Mechanics, 29.6–2.7.1998, Buenos Aires, Argentina* (CD-ROM), Part II, Section 7, Paper 16, 1–14, 1998.

[10] O.C. Zienkiewicz, R.L. Taylor. *The Finite Element Method*, Vol. 2, 4th edition. McGraw–Hill, London, 1989.